

Pulse Propagation in Resonant Tunneling

Ulrich Wulf¹ and V. V. Skalozub²

¹*Technische Universität Cottbus, Lehrstuhl für Theoretische Physik
and IHP/BTU Joint Lab, Postfach 101344, 03013 Cottbus, Germany*

²*Dnipropetrovsk National University, Dnipropetrovsk 49050, Ukraine*

(Dated: March 23, 2022)

We consider the analytically solvable model of a Gaussian pulse tunneling through a transmission resonance with a general Fano characteristic. It is demonstrated that the transmitted pulse contains enough information to determine uniquely all parameters defining the Fano resonance. This is in contrast to the measurement of the static conductance. Our analytical model is in agreement with numerical data published recently for the limit of a Breit-Wigner resonance. We identify two opposite pulse propagation regimes: if the resonance is broad compared to the energetic width of the incident Gaussian pulse a weakly deformed and slightly delayed transmitted Gaussian pulse is found. In the opposite limit of a narrow resonance the dying out of the transmitted pulse is dominated by the slow exponential decay characteristic of a quasi-bound state with a long life time. In this regime we find characteristic interference oscillations.

PACS numbers: 73.23.A, 03.65.Xp, 73.63.-b

I. INTRODUCTION

In a number of semiconductor nanosystems at low enough temperatures the ballistic transport properties are dominated by a single resonance. Well known examples are the double barrier resonant tunneling diode and quantum dots. Depending on the coupling of the dot to the contacts, one observes in the conductance of the latter systems Coulomb blockade oscillations, the Kondo effect, or Fano resonances^{1,2,3}. In the Fano regime strongly asymmetric conductance peaks as well as anti-resonances are observed^{2,4} which result from a coherent interaction of the resonance with a nonresonant background. In a previous paper⁵ an S-matrix analysis of these line shapes was derived: the resonance corresponds to a pole in the S-matrix in the 'unphysical' sheet of the complex energy plane⁶. A systematic linearization of the slowly varying parts of the S-matrix⁵ in the vicinity of this pole yields an expansion for the relevant real energies close to the center E_1 of the resonance as given by

$$S(E) = S_{res} \frac{i\frac{\Gamma}{2}}{E - E_1 + i\Gamma/2} + S_{bg} = S_{bg} \frac{\epsilon + q}{\epsilon + i}. \quad (1)$$

Here $S_{res} = S(E_1) - S_{bg}$ and $\epsilon = 2(E - E_1)/\Gamma$, where Γ is the width of the resonance. Since the pole strength S_{res} and the background transmission coefficient S_{bg} are independent from each other it is immediately clear that the asymmetry parameter $q = iS(E_1)/S_{bg}$ is complex in the generic case.

Applying the Landauer-Büttiker formalism one obtains from Eq. (1) Fano-type resonances in the stationary conductance⁵. In real experiments one has to add to this coherent conductance a noncoherent conductance background resulting from independent transmission channels (see, for example, Eq. (3) in Ref.² where a real q was assumed). These extra channels might either be coherent channels that do not couple to the resonant channel or independent incoherent transport channels. As a basic problem, it is known^{5,10,11}, that such a noncoherent conductance background has the same effect on the conductance than a coherent background term caused by S_{bg} . Therefore, in a fit of the stationary conductance with a general Fano profile a coherent conductance background S_{bg} cannot be resolved from a noncoherent conductance background. In consequence it is not possible to extract the parameters q and S_{bg} uniquely from a measurement of the stationary conductance.

To overcome the described problem of a stationary conductance measurement we analyze the pulse transmission properties in presence of a Fano resonance. Assuming a simple Gaussian incident pulse and the validity of Eq. (1) we obtain a first analytical description to cover the pulse transmission in the entire Fano resonance regime. Furthermore, in difference to previous calculations on resonant pulse transmission^{8,12,13,14,15,16,17,18,19} in our model the properties of the transmitted pulse can be related directly to the critical parameters q and S_{bg} . We demonstrate that in a pulse transmission experiment, one can distinguish between a resonant and a nonresonant conductance background making it possible to determine the parameters q and S_{bg} uniquely. However, at typical confinement lengths in the order of tens of nanometers we find typical times to resolve the needed shape of the transmitted pulses in the order of picoseconds. Such a time regime is very hard to achieve experimentally and we are not aware of any of such data.

In a system without background transmission our analytical results are in agreement with numerical calculations by Konsek and Pearsall¹³. Neglecting the coherent background term in Eq. (1) our model allows for a continuous

transition between the limits of a broad and a narrow resonance on scale of the energetic width of the incident packet: in the first case a weakly distorted Gaussian (WDG) transmitted pulse results with a small delay with respect to the unscattered pulse²⁰. In the limit of a narrow resonance considered by¹³ we find that the transmitted signal is dominated by the decaying state (DS) associated with the pole in Eq. (1). This DS corresponds to a solution of the stationary Schrödinger Equation with purely outgoing boundary condition and with the complex eigenenergy $E_1 - i\Gamma/2$ ^{7,8,9}. It is found that for narrow resonances the dropping flank of the transmitted pulse is not Gaussian any more but dominated by a slow exponential time characteristic $\propto \exp(-\Gamma/2t)$ associated with the complex part of the eigenenergy. In addition, there appear characteristic oscillations in space and time in the absolute value of the wave function of the transmitted pulse.

II. MODEL

We analyze a set-up as depicted in Fig. 1: an incident standard Gaussian wave packet

$$\psi_0(x, t) = \frac{\psi_0}{\sqrt{1 + i\frac{\hbar}{ma^2}t}} \exp\left[-\frac{(x - v_0t)^2}{2a^2(1 + i\frac{\hbar}{ma^2}t)}\right] \exp\left[ik_0x - i\frac{\hbar k_0^2}{2m}t\right] \quad (2)$$

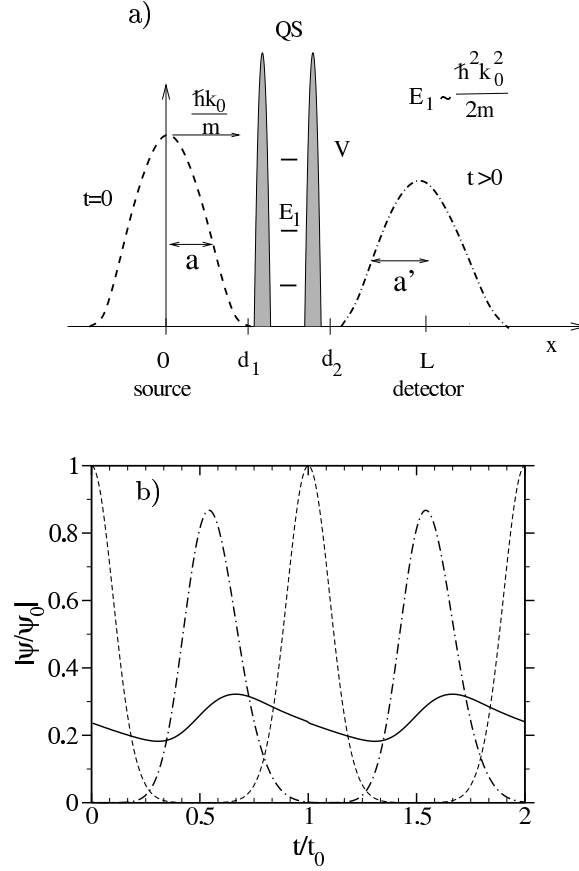


FIG. 1: Part (a): schematic representation of the incident Gaussian packet (dashed line) approaching the quantum system. The transmitted signal (dash-dotted line) is detected at $x = L$.

Part (b): absolute value of the wave function versus time. In dashed line the sequence of the incident pulses at $x = 0$. In dash-dotted line the quasi-stationary limit for the transmitted pulses detected at $x = L$ for $\rho = 2$ (broad resonance) and in solid line for $\rho = 0.1$ (narrow resonance). The further parameters are $L = 5a$, $k_0a = k_1a = 10$, and $|S_0| = 1$.

is approaching a tunneling barrier with a group velocity $v_0 = \hbar k_0/m$. At $t = 0$ the incident packet has a width of a in real space. The transmitted pulse is given by the expression

$$\psi(x > d_2, t) = \int_0^\infty \frac{dk}{\sqrt{2\pi}} \psi_0(k) S(k) \exp \left[ikx - i \frac{\hbar}{2m} k^2 t \right], \quad (3)$$

where $\psi_0(k)$ is the Fourier transform of $\psi_0(x, t = 0)$. A short range scattering potential is assumed so that $V(x) = 0$ outside the interval $d_1 \leq x \leq d_2$. Furthermore it is assumed that there is an isolated resonance at $E_1 \approx \hbar^2 k_0^2 / (2m)$, i. e. close to the mean kinetic energy of the incident pulse. Then in the range of finite $|\psi_0(k)|$ the transmission coefficient can be approximated by an expression

$$S(k) = S_0 \frac{i \frac{\Gamma_k}{2}}{k - k_1 + i \frac{\Gamma_k}{2}} + S_b, \quad (4)$$

with $S_0 = S(k_1) - S_b$. With the usual transformation $E = (\hbar^2/2m)k^2$ one can derive Eq. (4) from Eq. (1). Here one has to take into account that the representation of the S-matrix in the complex energy plane in Eq. (1) only holds for the lower part of the unphysical branch of the energy plane including the real axis, i. e. the imaginary part of the energy must be smaller than or equal to zero. In the complex k-plane this means $Re(k) \geq 0$ and $Im(k) \leq 0$ so that the entire integration range in Eq. (3) is covered. Comparing the denominators in the first factor on the right hand side of (4) and (1) one obtains the relations $k_1 = \sqrt{2mE_1}/\hbar$ and $\Gamma_k = (\hbar v_1)^{-1} \Gamma$, with $v_1 = \hbar k_1/m$ for $\Gamma/E_1 \ll 1$. Furthermore it results that

$$S_0 = \frac{\Gamma}{\Gamma_k} \frac{m}{\hbar^2} \frac{1}{k_1 - i \Gamma_k/2} S_{res}, \quad (5)$$

and

$$S_b = S_{bg} - \frac{S_0}{2} \frac{i \Gamma_k/2}{k_1 - i \Gamma_k/2}. \quad (6)$$

We define an asymmetry parameter of the Fano distribution in k-space as given by $q_k = iS(k_1)/S_b$. Combining Eqs. (3) and (4) an integral is obtained that can be solved analytically²¹,

$$\psi(x > 0, t) = S_0 \psi_0(x, t) \left[-\frac{1}{(1 + iq_k)} + \rho \sqrt{\pi \beta} \mathcal{F}(iz) \right]. \quad (7)$$

Sometimes the function \mathcal{F} with

$$\mathcal{F}(iz) = \exp(z^2) \text{erfc}(z) \quad (8)$$

is called Fadeeva function where erfc is the complementary error function. The argument z is given by

$$z = \left(\frac{q}{2\sqrt{\beta}} - i\gamma\sqrt{\beta} \right), \quad (9)$$

with $q = (x - v_0 t)/a$, $\beta = (1 + i\tau)/2$, $\tau = t/t_0$, $t_0 = ma^2/\hbar$, and $\gamma = a[k_0 - k_1 + i\Gamma_k/2] \equiv \Delta + i\rho$. The first factor in the square bracket in Eq. (7) results from the transmission background S_b in Eq. (4), the second term results from the resonant term in (4).

When the background term is neglected it is possible to formally relate Eq. (7) to the basic problem of the propagation of a step function modulated sine-signal in a dispersive medium^{22,23,24}. This model, initiated by Sommerfeld, is often invoked to discuss general features of signal transport. As an example we consider Ref.²³ where a dispersion of $\omega = 1 + k^2$ has been assumed. Because of the structural equivalence of Eq. (A1) of Ref.²³ and Eq. (3) the following mapping between the basic quantities results: the variable a in Eq. (A1) which is the time variable has to be identified with β in the present problem which is essentially the complex time. The variable b in Eq. (A1) which is the negative space coordinate has to be identified with q which is a mixture of space and time. Finally, the wave vector k_0 in Eq. (A1) which is purely imaginary for an evanescent medium (frequency in the gap) and purely real in a propagating medium (frequency in the band) has to be identified with γ . A systematic analysis of the relation between the present model and the Sommerfeld model using the saddle point method is left to a subsequent paper. Here we only emphasize that in the Sommerfeld model the whole signal transfer process is regarded to take place in the same medium which is represented by a complex refraction index. In our case there is a clear distinction between the sender domain, the transmission structure, and the receiver domain. As illustrated in Fig. 1 this distinction is inspired by the possible use of a resonant tunneling diode as a signal transmission structure, where the sender domain is provided by the source contact and the receiver domain by the drain contact.

III. RESONANCE WITHOUT BACKGROUND TRANSMISSION

We begin our analysis considering systems where the background transmission can be neglected, $|S_b| \ll |S(k_1)|$ and therefore $|q_k| \rightarrow \infty$. Then Eq. (7) becomes

$$\psi(x > 0, t) = S_0 \psi_0(x, t) \rho \sqrt{\pi \beta} \mathcal{F}(iz). \quad (10)$$

From (10) it follows that the wave function as a function of q and τ depends only on the complex parameter γ apart from the global transmission coefficient S_0 . In this paper $\gamma = i\rho$ is chosen purely imaginary. Depending on the parameter ρ two different pulse propagation regimes result from Eq. (10). They are illustrated in Fig. 1(b). Here we plot the transmitted signal in the stationary state resulting from a sequence of well separated incident Gaussian pulses which are created at integer $t/t_0 = n$ with the center in real space at $x = 0$. For the broad resonance ($\rho > 1$) the transmitted pulse at $x = L$ is a sequence of well separated WDG pulses. These pulses arrive with a small delay with respect to the times $t/t_0 = n + 1/2$ at which the signal without scattering potential would arrive. In contrast, if the resonance is narrow ($\rho \ll 1$) the transmitted pulses are strongly weakened and deformed so that they are not separable any more. We will show below the reason for this drastic degradation of the signal transfer: for a narrow resonance the signal is dominated by the slow exponential time characteristic of the DS with a life time that exceeds the time interval of two subsequent pulses.

The parameters used for the calculations in Fig. 1(b) have been chosen to demonstrate that a nearly optimal signal transfer rate can be achieved for a broad resonance. We call a signal transfer rate (number of detected pulses at $x = L$ per time) optimal under the following conditions: first, the input pulses follow each other in a minimum time interval to allow for a separation at $x = 0$, second, the output pulses are still well separable at $x = L$, and, third, the attenuation of the pulses is low when passing from $x = 0$ to $x = L$. To achieve this goal the following design rules have been applied: i.) the detector at $x = L$ is positioned in a minimum distance of $L \approx 5 \div 10a$ from the source at $x = 0$. As illustrated in Fig. 1(a) this choice results from the requirements, first, that when the pulse is prepared or detected it should be well separated from the resonant tunneling structure and, second, that the spatial width of the signal is assumed to be comparable in size to the tunneling structure. ii.) the traveling time of the signal which is the time the maximum of a given pulse needs to pass $x = L$ should not exceed the characteristic time $t_0 = ma^2/\hbar$ of the quantum spread of the free wave packet in Eq. (2). For an electron packet with a width of $a = 10nm$ this time is very short, $t_0 \approx 10^{-12}s$. We can therefore define a minimum speed $v_{min} = L/t_0 = \hbar k_{0,min}/m$ which defines a minimum central position $k_{0,min}$ of the Gaussian peak in k -space (we neglect here the spread induced by the Coulomb interaction). iii.) for a maximum signal intensity we require $k_0 = k_1$ ($\Delta = 0$) which is optimal resonance. iv.) the imaginary part of the resonance energy is fixed by the condition $\rho > 1$ with the constraint that the resonance should still be isolated. v.) for an effectively symmetrical double barrier structure the absolute value of S_0 is very close to unity²⁵. Apart from iv.) these rules are met in the on-resonance calculations in Ref.¹³. Here we find $\rho \sim 0.1 < 1$ as in the system represented by solid lines in Fig. 1(b).

A detailed comparison of the pulse propagation properties in the regime of broad resonances and in the regime of narrow resonances is contained in Fig. 2 and Fig. 3. We will demonstrate that the basic differences can be understood in a proper expansion of the complementary error function in Eq. (10). As shown in Fig. 2 for a broad resonance Eq. (10) describes a WDG pulse. In this case we find in the relevant q -range (q values for which $|\psi|$ deviates significantly from zero) that the absolute value of z is relatively large and that the argument of z is less than $3\pi/4$ (see Figs. 2 (b) and (c)). Under this condition we can introduce an asymptotic z expansion of the error function as given in²⁶ yielding

$$\psi(x, t) = S_0 \frac{\rho \sqrt{\beta}}{z} \left[1 + \sum_{m=1} \frac{a_m}{(2z^2)^m} \right] \psi_0(x, t) \equiv \psi_{WDG}(x, t), \quad (11)$$

with $a_m = (-1)^m [1 \times 3 \times 5 \dots \times (2m-1)]$. The expression in Eq. (11) clearly reveals the WDG character of the transmitted pulse: the weak distortion of the incident Gaussian pulse $\psi_0(x, t)$ follows, first, from the fact that at large ρ the parameter $1/(2|z|^2)$ is small compared to unity. Therefore, the second term in the square bracket in Eq. (11) gives only a small correction. In fact, only the first two terms in the sum over m in Eq. (11) are necessary to approximate the analytical result from Eq. (10) within plot resolution. Second, for large ρ the argument z depends only very weakly on q . This explains that the factor $1/z$ in front of the square bracket in Eq. (11) merely leads to a minor deformation of the packet as well. Note that in the illustrated example $\rho = 2$ takes a moderate value and that the approximation in Eq. (11) works even better for larger ρ for a small amount of terms in the m summation.

An inspection of Fig. 3 (a) shows immediately that for a narrow resonance the unperturbed incident Gaussian pulse is no good approximation for the transmitted pulse. The difference is most pronounced for short times. For example, at $\tau = 1$ a narrow Gaussian transmitted peak results in the case of a broad resonance (Fig. 2 (a)) while for the narrow

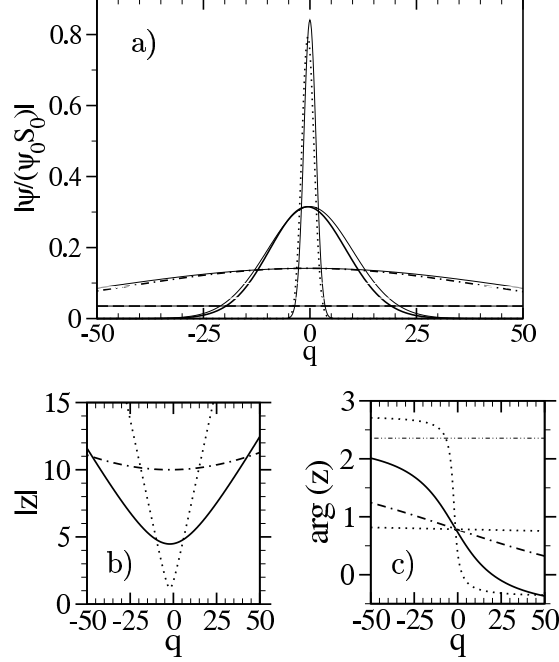


FIG. 2: Part a): Absolute value of the transmitted wave function for a broad resonance with $\rho = 2.0$ at $\tau = 1.0$ (dotted line), $\tau = 10$ (solid line), $\tau = 50$ (dash-dotted line), and $\tau = 800$ (dotted line). Thick lines represent the exact result in Eq. (7) and, for comparison, thin solid lines the result for $\psi = \psi_0(x, t)$ in Eq. (2). For $\tau = 800$ the corresponding lines are not resolvable. Part b) absolute value of z (see Eq. (9)) and part c) $\arg(z)$ with the same line-coding as in part a). The thin dash-dot-dotted line in (c) represents $\arg(z) = 3\pi/4$.

resonance (Fig. 3 (a)) a much weaker, broader, and strongly asymmetric resonance results which is nearly completely restricted to negative q . To explain the difference we observe that for the broad resonance the argument of z is smaller than $3\pi/4$ in the relevant q -range of the transmitted peak ($-5 \leq q \leq 5$ at $\tau = 1$, see Figs. 2 (b) and (c)). In contrast, for the narrow resonance the argument of z is larger than $3\pi/4$ in the relevant q -range of the transmitted peak ($q \leq 0$ see Figs. 3 (a) and (c)). To obtain for small ρ an approximate expression for $q \leq 0$ one expands $\text{erfc}(-z)$ according to²⁶ instead of $\text{erfc}(z)$ as has been done for the broad resonance. Then, a superposition of *two* factors

$$\psi(x, t) = \psi_{WDG}(x, t) + \psi_{DS}(x, t), \quad (12)$$

is obtained with

$$\psi_{DS}(x, t > 0) = \psi_0 S_0 \rho \sqrt{2\pi} \exp(\beta \rho^2) \exp\left[\frac{\Gamma_k}{2}(x - v_0 t)\right] \exp\left(ik_0 x - i\frac{\hbar k_0^2}{2m}t\right). \quad (13)$$

For the narrow resonance the factor $\psi_{DS}(x, t > 0)$ is the dominant contribution to the signal and $\psi_{WDG}(x, t)$ is small. The dominant factor ψ_{DS} results from a DS. This can be seen, first, from the exponential decay $\propto \exp(-\Gamma t/2)$ with $\Gamma = v_0 \Gamma_k$ at a fixed space coordinate x . Second, at a fixed time the wave function grows $\propto \exp(\Gamma_k x/2)$ which is typical for a DS⁷. This growth continues up to $q \approx 0$ where the wave front of the decaying state signal is located. As can be gathered from Fig. 3 (b) this wave front can well be described by replacing in Eq. (7) the complementary error function by its small z -expansion $1 - 2z/\sqrt{\pi} + \dots$ ²⁶.

In Fig. 3 (a) the curve for $\tau = 10$ shows characteristic oscillations superimposed to the decaying state signal which are presented in more detail in Fig. 4. For $q \leq -8$ the exact result from Eq. (10) agrees within plot resolution with the approximations in Eqs. (11) - (13) (the sum over m in Eq. (11) can be neglected). The latter equations demonstrate the origin of the oscillations. They are caused by the interference between the dominant component ψ_{DS} and the small component ψ_{WDG} . Here the oscillating phase is in the Gaussian factor $\exp[-q^2/(4\beta)]$ in ψ_{WDG} at complex β .

To show this we introduce further approximations in Eq. (11): first, for moderate times $\tau \sim 10$ one may set $\beta \sim i\tau/2$ outside the Gaussian factor $\exp[-q^2/(4\beta)]$ and, second, for small ρ the contribution $\rho\sqrt{\beta}$ in z can be omitted. It results that

$$\psi_{WDG} = S_0\psi_0 \frac{\sqrt{\tau}}{q} \rho \exp\left(-\frac{q^2}{4\beta} + i\frac{\pi}{4}\right) \exp\left[ik_0x - i\frac{\hbar k_0^2}{2m}t\right]. \quad (14)$$

With this approximation for ψ_{WDG} and with Eq. (13) a representation $|\psi(x, t)| = |\psi_{DS}(x, t)| + \psi_{OSZ}(x, t)$ follows where

$$\psi_{OSZ} = \frac{\text{Re}(\psi_{DG}\psi_{DS}^*)}{|\psi_{DS}|} = -|\psi_0 S_0| \rho \frac{\sqrt{\tau}}{q} \exp\left(-\frac{q^2}{2(1+\tau^2)}\right) \sin\left(\frac{q^2}{2\tau} - \frac{\tau}{2}\rho^2 - \frac{\pi}{4}\right). \quad (15)$$

As shown in in Fig. 4 this expression describes the characteristic oscillations very accurately. Apart from the constant phase $-\pi/4$ the argument in the sine-factor in Eq. (15) stems from $\exp[-q^2/(4\beta)]$ in Eq. (14). This argument determines solely the phase and the period of the characteristic oscillations.

In Fig. 4 we represent numerical data taken from Konsek and Pearsall for the 'on-resonance' wave packet as given in Fig. (3) of Ref.¹³. To include these data in Fig. 4 we read off from Fig. 2 (a) in Ref.¹³ the values $a = 2nm$ and $|\psi_0| = \sqrt{28 \times 10^{-3}} = 0.167$ for the incident Gaussian packet. From Fig. 2 (b) we estimate for the width of the resonance the value $\Gamma = 25meV$. For the 'on-resonance' wave packet ($\Delta = 0$) the center of the resonance is given by $E_0 = \hbar^2 k_0^2/(2m)$, where $\hbar k_0/m = v_0$ and $v_0 = 4.1 \times 10^5 ms^{-1}$ is the speed of the unscattered Gaussian package. We find $\rho = a\Gamma_k/2 = a\Gamma/(2\hbar v_0) = 0.092$. After having been prepared at $t = 0$ the shape of the wave packet is determined numerically at a time $t = 5 \times 10^{-14}$ so that $\tau = 1.44$. The parameter pair $\rho = 0.092$ and $\tau = 1.44$ is actually very close to the parameter pair $\rho = 0.1$ and $\tau = 1.0$ for which the exact result is plotted in Fig. 3 (dotted line). It follows immediately that we can describe the transmitted wave packet in Ref.¹³ with Eq. (12). Because of the small time τ one has a dominant DS component (Eq. (13)) while the WDG component in the transmitted signal is nearly negligible. Then no characteristic oscillations as in Eq. (15) appear. The small differences between our analytical

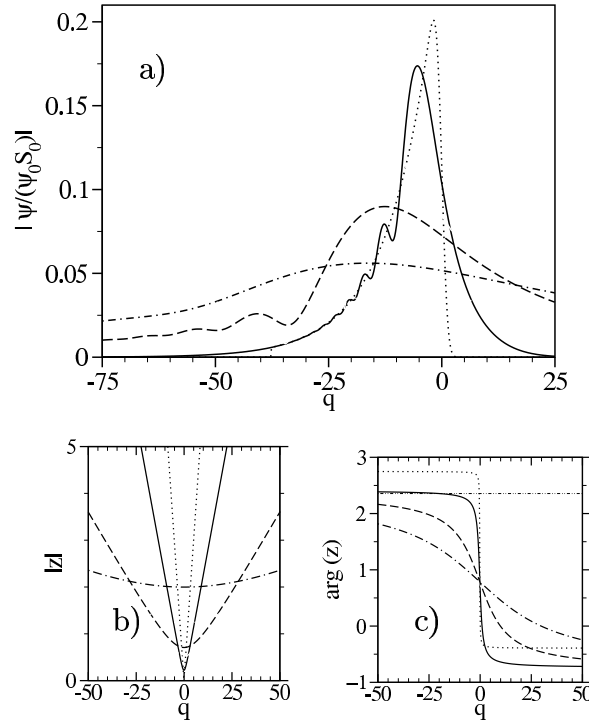


FIG. 3: (a) Absolute value of the transmitted wave function, (b) absolute value of z , and (c) the argument of z at $\rho = .1$, $l_1 = l_0$ $\tau = 1.0$ (dotted line), and $\tau = 10$. (solid line), $\tau = 100$ (dashed line), and $\tau = 300$ (dash-dotted line). The thin dash-dot-dotted line in c represents $\arg(z) = 3\pi/4$.

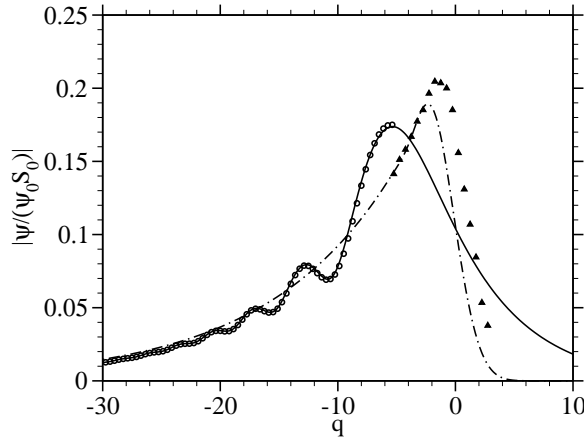


FIG. 4: Solid line exact result for $\rho = 0.1$ and $\tau = 10$ (see Fig. (3)) and in open circles approximation $|\psi| = |\psi_{DS}| + \psi_{OSZ}$ with ψ_{OSZ} as given in Eq. (15). Dash-dotted line exact result for $\rho = 0.092$ and $\tau = 1.44$ and triangles numerical results for this case taken from Ref.¹³ (see text). For the representation of the numerical results we set $q = x - x_0 - v_0 t$, where $x_0 = 50nm$ is the position of the center of the incident numerical packet at $t = 0$.

result and the numerical result by Konsek and Pearsall can be attributed to imprecisions in our determination of Γ and to deviations of the numerical line shape from the Breit-Wigner profile. One source for such a deviation is the existence of a background transmission. The effect of a background transmission will be discussed in the next section.

IV. RESONANCE WITH A BACKGROUND TRANSMISSION

In this section we want to demonstrate that in the presence of a background transmission a pulse transmission experiment can yield valuable information about the scattering potential beyond the measurement of the stationary conductance. To be specific we focus on the case of an anti-resonance with $|q_k| \ll 1$. Furthermore, the anti-resonance is assumed to be broad compared to the incident Gaussian pulse, $\rho \geq 1$. We begin our analysis considering the static transmission calculated from Eq. (4) which is given by

$$T(k) = |S(k)|^2 = T_b \frac{[\kappa + \text{Re}(q_k)]^2 + \text{Im}(q_k)^2}{\kappa^2 + 1} + T_{of}, \quad (16)$$

with $\kappa = (k - k_1)/(\Gamma_k/2)$ and $T_b = |S_b|^2$. The static transmission of a typical anti-resonance resulting from Eq. (16) for $T_{of} = 0$ is illustrated in Fig. 5 (a). There is a pronounced dip for small $|\kappa|$ which produces a transmission zero at $\kappa = -q_k$ for real q_k . If a small imaginary part is introduced in q_k the transmission shows only a minimum, i. e. there is a residual transmission close to the position of the transmission zero at real q_k . Like in Ref.² (see Eq. (3) therein) we added in Eq. (16) a constant background term T_{of} to take into account the contribution of nonresonant independent transmission channels. These channels might either be coherent channels that do not couple to the resonant channel or independent incoherent transport channels. We therefore call T_{of} a noncoherent conductance background (noncoherent with respect to the resonant channel). However, in difference to Ref.² the coherent contribution in Eq. (16) which causes the resonance is represented with a complex asymmetry parameter q_k . In Ref.⁵ we have shown that such a complex asymmetry parameter q_k is the generic result for a general system. Now, if one applies Eq. (16) to the interpretation of experimental conductance peaks there arises a central problem: as illustrated in Fig. 5 there is a one-dimensional manifold of choices for the four parameters $T_b, T_{of}, \text{Re}(q_k), \text{Im}(q_k)$ leading to the same function $T(k)$ in Eq. (16). Therefore, if only $T(k)$ is determined by measuring the static conductance only three independent parameters can be determined in a fit procedure. We choose these parameters as T_b^F, T_{of}^F , and q_F with real q_F which result from a fit of the expression

$$T(k) = T_b^F \frac{(\kappa + q_F)^2}{\kappa^2 + 1} + T_{of}^F. \quad (17)$$

Such an expression was used in Ref.² to fit Fano-type conductance resonances in quantum dots in the strong coupling regime. However, at complex q_k the factor T_{of}^F cannot be taken as the contribution of the noncoherent channels. This

is demonstrated if one inserts in Eq. (16) the transformation

$$T_b = T_b^F + \alpha T_{of}^F, \quad (18)$$

$$Re(q_k) = q_F \frac{T_b^F}{T_b^F + \alpha T_{of}^F}, \quad (19)$$

$$Im(q_k) = \frac{T_{of}^F}{T_b^F + \alpha T_{of}^F} \sqrt{\alpha^2 + (1 + q_F^2) \alpha \frac{T_b^F}{T_{of}^F}}, \quad (20)$$

and

$$T_{of} = (1 - \alpha) T_{of}^F, \quad (21)$$

with the real parameter α chosen freely within the interval $0 \leq \alpha \leq 1$. This transformation leaves the function $T(k)$ invariant. For $\alpha = 1$ one recovers Eq. (16) and for $\alpha = 0$ one obtains Eq. (17). From Eq. (21) it follows that any measured fit parameter T_{of}^F is compatible with zero contribution of noncoherent channels, $T_{of} = 0$, if one takes $\alpha = 1$. Then the measured minimum conductance originates completely from the complex part of the asymmetry parameter. On the other hand a measured fit parameter T_{of}^F is maximally compatible with a contribution of noncoherent channels as given by $T_{of} = T_{of}^F$. In this special case the asymmetry parameter is real and $\alpha = 1$.

In the following we want to demonstrate that in principle it is possible to determine α with a combination of experiments on pulse transmission and on static transport. Here a measurement of $\alpha \neq 1$ would provide evidence for the correctness of Eq. (16). In Fig. 5 (b) results for the density n_{tot} of the total transmitted pulse are plotted with

$$|n_{tot}(x, t)|^2 = T_{of} |\psi_0(x, t)|^2 + |\psi(x, t)|^2. \quad (22)$$

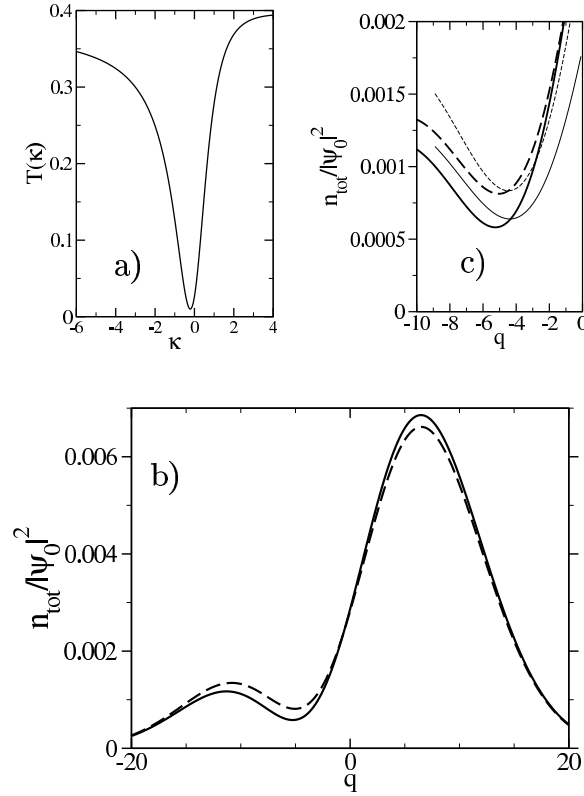


FIG. 5: a) Identical static transmission for $T_b = 0.38$, $T_{of} = 0$, $Re(q_k) = 0.195$, $Im(q_k) = 0.165$ [$\alpha = 1$, Eq. (16)] and for $T_b^F = 0.37$, $T_{of}^F = 0.01$, $q_F = 0.2$ [$\alpha = 0$, Eq. (17)]. b) Total transmitted pulse with the two resonances in a): $\alpha = 1$ (solid line, $|S_0|^2 = 0.28$) and $\alpha = 0$ (dashed line, $|S_0|^2 = 0.385$) at $\tau = 10$, $\rho = 2$, $\Delta = 0$. c) Detail of b). Thin lines approximation in Eq. (24).

Here the first factor arises from the constant noncoherent background transmission of the incident pulse $\psi_0(x, t)$. The second factor is given by the independent coherent transmission of the pulse via the resonant channel with a static transmission coefficient as given by Eq. (4). The wave function intensity coming from the coherent transmission component is the absolute square of Eq. (7). The parameters $|S_0|^2$, $|\psi_0|^2$, q_k , ρ , and τ which enter in the absolute square of Eq. (7) as a function of q we obtain in the following way: first, we assume that from a fit of the experimental static conductance according to Eq. (17) the parameters k_1 and Γ_k are known so that the incident packet can be prepared, for example, at $\Delta = 0$ and $\rho = 2 > 1$ (broad resonance, see Fig. 5). Second, from the fit of the static conductance the parameters T_b^F , T_{of}^F and q_F can be found. These three parameters fix according to Eqs. (19) and (20) a range of possible T_b , T_{of} , and complex q_k which is parametrized by α . Then, it follows easily that

$$|S_0|^2 = T_b \{[1 - \text{Im}(q_k)]^2 + \text{Re}(q_k)^2\}. \quad (23)$$

Third, to keep the analysis simple we consider in our theory the transmitted packet at a constant time which we choose to be relatively short, $\tau = 10$, so that particular features are not washed out in the time evolution. Fourth, we observe that both factors on the right hand side of Eq. (22) are proportional to the square to the parameter $|\psi_0|$ so it can be accounted for as a normalization parameter. In Fig. 5(b) we compare the transmitted pulse calculated from Eq. (22) for $\alpha = 1$ and for $\alpha = 0$. As a qualitatively new feature we find that in both cases there appears a pronounced dip in n_{tot} close to the center the pulse. As demonstrated in Fig. 5(c) this dip can be explained inserting in Eq. (22)

$$\psi(x, t) = S_0 \psi_0(x, t) i \left[q_k + \frac{q}{\rho \tau} \right], \quad (24)$$

valid for $|q/(\rho\beta)| \ll 1$. The expression in Eq. (24) can be derived from Eq. (7) approximating in the first factor in the square bracket $1/(iq_k + 1) \approx 1 - iq_k$ and introducing in the second factor Eq. (11) where we have dropped the qualitatively irrelevant summation over m . Finally like for Eq. (15) we have assumed moderate times so that $\beta \approx i\tau/2$. From Eq. (24) a minimum in n_{tot} follows at the position $q = -\rho\tau \text{Re}(q_k)$. As can be seen from Figs. 5(b) and (c) there are differences in the transmitted pulse at $\alpha = 1$ and $\alpha = 0$ making a determination of α possible. These differences are most pronounced in the region of the dip: the minimum of the absolute square of the wave function associated with the dip is about 25% smaller for $\alpha = 1$ than for $\alpha = 0$. Because of the spatial propagation of the transmitted pulses this effect also exists when the pulse is measured as a function of time in an appropriate position in space. Therefore, in principle, with a measurement of the minimum of the transmitted pulse associated with the dip it is possible to determine α . A pulse measurement can therefore resolve uncertainties in α resulting in a sole measurement of the static conductance.

V. CONCLUSIONS

We have analyzed an analytical model for the resonant transmission of a Gaussian wave packet. At zero background transmission and in the limit of a broad resonance a weakly distorted transmitted pulse results. In the opposite limit of a narrow resonance the transmitted wave is dominated by a decaying state and characteristic oscillations result. Our model also describes pulse transmission in presence of a coherent and a noncoherent transmission background. In this case the transmission is described by a general Fano profile. We focus on the case of an anti-resonance. We demonstrate that the characteristic effect of the transmission background is the formation of dips in the profile of the transmitted pulse. It is shown that the measurement of the pulse transmission in addition to static transport opens the possibility to distinguish between a coherent and a noncoherent conductance background. This distinction is clearest when the dip in the pulse profile is considered.

We acknowledge helpful discussions with D. Robaschik and P. Racec.

-
- ¹ D. Goldhaber-Gordon, J. Göres, M. A. Kastner, H. Shtrikman, D. Mahalu, and U. Meirav, Phys. Rev. Lett. **81**, 5225 (1998).
 - ² J. Göres, D. Goldhaber-Gordon, S. Heemeyer, M. A. Kastner, H. Shtrikman, D. Mahalu, and U. Meirav, Phys. Rev. B **62**, 2188 (2000).
 - ³ I. G. Zacharia, D. Goldhaber-Gordon, G. Granger, M. A. Kastner, Yu. B. Khavin, H. Shtrikman, D. Mahalu and U. Meirav, Phys. Rev. B **64**, 155311 (2001).
 - ⁴ C. Fühner, U. F. Keyser, R. J. Haug, D. Reuter, and A. D. Wieck, Phys. Stat. Sol. (C) **4**, 1305 (2003).
 - ⁵ E. R. Racec and U. Wulf, Phys. Rev. B **64**, 115318 (2001).

- ⁶ A. Bohm, *Quantum mechanics: foundations and applications*, (Springer, New York, 1994).
- ⁷ A. M. Perelomov and Y. B. Zel'dovich, *Quantum mechanics - selected topics*, (World Scientific, Singapore, 1998)
- ⁸ J. A. Støvneng and E. H. Hauge, Phys. Rev. B **44**, 13582 (1991).
- ⁹ M. Wagner and H. Mizuta, Phys. Rev. B **48**, 14393 (1993).
- ¹⁰ G. Abstreiter, M. Cardona, and A. Pinczuk in *Light Scattering in Solids*, edited by M. Cardona and G. Güntherodt, Topics in Applied Physics Vol. 54 (Springer, Berlin, 1984), p.127.
- ¹¹ K. J. Jin, S. H. Pan, and G. Z. Yang, Phys. Rev. B **50**, 8584 (1994).
- ¹² J. Villavicencio and R. Romo, Phys. Rev. B **68**, 153311 (2003).
- ¹³ S. L. Konsek and T. P. Pearsall, Phys. Rev. B **67**, 45306 (2003).
- ¹⁴ H. P. Simanjuntak and P. Pereyra, Phys. Rev. B **67**, 045301 (2003).
- ¹⁵ R. Romo, J. Villavicencio and G. García-Calderón, Phys. Rev. B **66**, 33108 (2002).
- ¹⁶ Ph. Grossel, F. Depasse and J.-M. Vigoureux, J. Phys. A **35**, 9787 (2002).
- ¹⁷ P. Pereyra, Phys. Rev. Lett. **84**, 1772 (2000).
- ¹⁸ *The Physics and Applications of Resonant Tunneling Diodes*, H. Mizuta and T. Tanoue, (Cambridge University press, Cambridge, 1995).
- ¹⁹ N. Harada and S. Kuroda, Jpn. J. Appl. Phys. **25**, L871 (1986).
- ²⁰ F. S. Levin, *An Introduction to Quantum Theory*, (Cambridge University Press, Cambridge, 2002).
- ²¹ We used the basic integrals 3.954 in *Table of Series, Products, and Integrals*, I. S. Gradshteyn, I. M. Ryzhik, A. Jeffrey, Yu. V. Geronimus, and M. Yu. Tseytlin (Academic Press, San Diego, 1980).
- ²² L. Brillouin, *Wave propagation and group velocity*, (Academic Press, New York and London, 1960).
- ²³ J. G. Muga and M. Büttiker, Phys. Rev. A **62**, 23808 (2000).
- ²⁴ A. Ruschhaupt and J. G. Muga, Phys. Rev. Lett. **93**, 20403 (2004).
- ²⁵ P. N. Racec, T. Stoica, C. Popescu, M. Lepsa, and Th. G. van de Roer, Phys. Rev. B **56**, 3595 (1997).
- ²⁶ M. Abramowitz and I. Stegun, *Handbook of Mathematical Functions*, (Dover Publications, New York, 1970), expansion for large z see 7.1.23 and for small z see 7.1.5.